Journal of Applied Physics ARTICLE scitation.org/journal/jap

Atomistic origin of compositional pulling effect in wurtzite (B, Al, In)$_x$Ga$_{1-x}$N: A first-principles study

Cite as: J. Appl. Phys. **130**, 035704 (2021); doi: 10.1063/5.0050102
Submitted: 12 March 2021 · Accepted: 28 June 2021 ·
Published Online: 16 July 2021

View Online

Export Citation

CrossMark

Hiroshi Mizuseki,[1,a)] Jessiel Siaron Gueriba,[2] Melvin John F. Empizo,[2] Nobuhiko Sarukura,[2] Yoshiyuki Kawazoe,[3,4,5] and Kazuhiro Ohkawa[6]

AFFILIATIONS

[1]Korea Institute of Science and Technology (KIST), Seoul 02792, Republic of Korea
[2]Institute of Laser Engineering, Osaka University, 2-6 Yamadaoka, Suita, Osaka 565-0871, Japan
[3]New Industry Creation Hatchery Center, Tohoku University, Sendai, 980-8579, Japan
[4]SRM Institute of Science and Technology, SRM Nagar, Kattankulathur, Kancheepuram District, Tamil Nadu 603 203, India
[5]School of Physics, Institute of Science and Center of Excellence in Advanced Functional Materials, Suranaree University of Technology, Nakhon Ratchasima 30000, Thailand
[6]Computer, Electrical and Mathematical Sciences and Engineering Division, King Abdullah University of Science and Technology (KAUST), Thuwal 23955-6900, Saudi Arabia

[a)]**Author to whom correspondence should be addressed:** mizuseki@kist.re.kr

ABSTRACT

Some fluctuations in composition are commonly observed in epitaxial-grown III-V multinary alloys. These fluctuations are attributed to compositional pulling effects, and an insight into their atomistic origin is necessary to improve current epitaxial growth techniques. In addition, the crystallinity of III-V multinary alloys varies widely depending on the constituent atoms. Using first-principles calculations, we then investigated different geometric configurations of gallium nitride (GaN)-based ternary alloy, $X_{0.125}Ga_{0.875}N$ where X is the minority atom which is boron (B), aluminum (Al), or indium (In). The minority atoms are presented as two atoms in the simulation cell, and the energetics of five geometric configurations are analyzed to estimate the most stable configuration. For the $B_{0.125}Ga_{0.875}N$ alloy, the most stable configuration is the one where the minority atoms occupy gallium (Ga) sites in a collinear orientation along the c-axis. On the contrary, the configurations along the in-plane direction result in a higher energy state. $In_{0.125}Ga_{0.875}N$ and $Al_{0.125}Ga_{0.875}N$ also show the same trend with a small relative energy difference. These preferential sites of minority atoms are consistent with composition pulling effects in wurtzite nitride phases. Moreover, the degree of crystallinity for wurtzite nitride alloys can be well described by the order of calculated relative energy.

Published under an exclusive license by AIP Publishing. https://doi.org/10.1063/5.0050102

I. INTRODUCTION

Semiconductor bandgap engineering is vital for optoelectronics technologies as bandgap engineering involves fine-tuning the desired bandgap as well as obtaining transitions for specialized applications. In altering material properties, it has been known that the presence of minority atoms in semiconductor alloys induces geometrical deformations and consequently affects the alloy electronic structure. With the currently available fabrication techniques, these deformations and defects are hardly non-existent and may give rise to a variety of optical and electrical phenomena. In the case of epitaxial growth, the fabricated layer may exhibit a variety of compositional configurations due to the lattice mismatch with the substrate, thus affecting its viability for a specific application. This effect is widely present in multinary systems such as the technologically important III-nitride semiconductors.

III-nitride semiconductors are used in a wide range of applications such as field-effect transistors, solar cell materials, and optoelectronic devices.[1–3] In the last few decades, a large number of more complicated multinary systems or alloys have been produced and have been utilized because of their physical properties.[4–7] Moreover, III-nitride multinary alloys have become promising candidate materials for deep ultraviolet (DUV) to near-infrared (NIR) applications by just varying the composition of the group III elements. Optical devices such as light-emitting diodes (LEDs) and

Published under an exclusive license by AIP Publishing

laser diodes (LDs) have then been realized owing to the intrinsic characteristics of III-nitride semiconductors.[8–12] However, in order to maximize the performance of these materials, it is necessary to produce high-quality crystals with low defect density.

Despite the different applications of III-nitride multinary alloys, the challenges in growth and manufacturing have led to semiconductor alloys with a wide degree of crystallinity. The crystallinity of epitaxial layers has been investigated and has been evaluated using the threading dislocation density (TDD). Amano reported that the TDD of an AlGaN superlattice on a sapphire substrate is less than $1 \times 10^{10}\,\mathrm{cm}^{-2}$.[13] Sugiyama *et al.* also measured the TDD of a single $In_{0.17}Ga_{0.83}N$ layer and $In_{0.17}Ga_{0.83}N/In_{0.07}Ga_{0.93}N$ superlattices on a GaN substrate and found that the TDD of superlattices was $5 \times 10^{7}\,\mathrm{cm}^{-2}$, while that of the single $In_{0.17}Ga_{0.83}N$ layer is two orders of magnitude higher.[14] On the other hand, it has been shown that AlN and AlGaN containing B exhibit low crystallinity. Gunning *et al.* fabricated $B_xGa_{1-x}N$ on GaN and AlN substrates and obtained a structure that contains high-density stacking faults.[15] In addition, Rettig *et al.* reported phase separation and columnar growth in $B_{0.05}Al_{0.95}N$ as well as stacking faults and edge dislocations in AlBGaN/AlN superlattices containing 1% B wherein only a few layers of such superlattice structure can be maintained.[16] From the available experimental results, there is a large difference in the crystallinity among III-nitride multinary alloys in which B, Al, and In atoms occupy the Ga sites in GaN and TDD is used as a criterion. However, the atomistic origin and factor that can explain these differences in the crystallinity in relation to the constituent atoms are still unclear.

Composition pulling effect, a phenomenon where the fabricated layer is affected by the substrate composition, has often been observed during epitaxial growth. This phenomenon becomes an obstacle in forming a uniform crystal structure with a specific composition.[17] Composition pulling effect is affected greatly by the incorporation rate, wherein the incorporation rate of minority atoms into the epitaxial layer is influenced by the composition of the substrate or the subsurface layer. For instance, Karasawa *et al.* pointed out that the incorporation rate is closely related to the degree of lattice mismatch wherein, as a typical example, lattice mismatch in atomistic scale also affects macroscopic constituent composition.[18] Furthermore, insights into a spatial relationship between the minority atoms, particularly in a wurtzite GaN crystal structure, have not been obtained experimentally but can be observed through computational investigations.

With the aid of recently developed high-performance computing facilities, many theoretical methodologies emerged to predict the physical properties of III-V semiconductors using first-principles calculations. Several first-principles studies focus on the effect of alloy fraction of the minority atoms on the electronic, thermal, and mechanical properties of semiconductors.[19–24] However, for a specific alloy concentration, non-degenerate configurations may arise resulting in more property variations for a single alloy concentration. Studies on the atomic ordering of III-nitride semiconductors show how the arrangement of minority atoms is necessary to obtain ground state structures for specific concentrations. They also show that atomic ordering affects the bandgap bowing parameter for semiconductor alloys.[25,26] Hence, in this work, we show the energetics of different spatial configurations for low concentration (12.5%) minority atoms in a III-nitride semiconductor with B, Al, and In as minority atoms. In this regard, large-scale first-principles calculations with a supercell scheme are performed to investigate the influence of substitutional B, Al, and In atoms on the strain and the energetics of a GaN-based ternary alloy. First-principles calculations using a $2 \times 2 \times 2$ supercell are applied to reveal the spatial relationship between minority atoms and their effect on the wurtzite GaN-based alloy crystal structure. We then show how the relative energies of the atomic configurations are influenced by the lattice mismatch relative to GaN and in effect initiates compositional pulling.

II. CALCULATION METHODS

We performed density functional theory (DFT) calculations[27] implemented by the Vienna *ab initio* simulation package (VASP).[28,29] The Perdew–Burke–Ernzerhof (PBE) exchange-correlation functional[30] was chosen for electronic structure calculations and geometry relaxation. The electron–ion interaction was described by the full-potential all-electron projector augmented wave (PAW) method.[31,32] The Brillouin zone was described by a set of k-points in a $15 \times 15 \times 7$ grid mesh using the Monkhorst–Pack method.[33] The plane-wave basis set with a kinetic energy cutoff of 600 eV was set to describe electron wave functions. Convergence tests were performed to obtain the optimal values for both k-points and energy cutoff (cf. Tables S3 and S4 in the supplementary material). For structural optimization, we used conjugate-gradient method until the absolute value of the components of the Hellman–Feynman forces was converged within 0.001 eV/Å. The optimized configurations were also drawn using VESTA software.[34]

To evaluate the physical properties of alloys, conventional first-principles calculations usually use the minimum calculation cell size that can reproduce the crystal structure. In the case of a small composition rate of a specific element, only one atom as a minority element is set in the calculation cell. In these calculation conditions, the spatial configurations among minority atoms are limited by the size of the supercell. However, the energetics of compounds are strongly dependent on the configuration of minority atoms within the crystal. Hence, it can be difficult to examine the difference in properties caused by varied configurations of the minority atoms using a small unit cell model. Therefore, investigations in the atomic ordering of minority atoms in semiconducting alloys using a relatively large supercell are essential.

In this study, we used a $2 \times 2 \times 2$ supercell to estimate the most stable configuration of the B, Al, and In as minority atoms in a GaN-based ternary alloy. Two minority atoms occupied the Ga sites in a wurtzite GaN crystal lattice translating to an alloy fraction of 12.5%, i.e., $X_{0.125}Ga_{0.875}N$ with $X = $ B, Al, or In. With a relatively small supercell used for energy comparison, we defined five inequivalent configurations for two minority atoms in the $2 \times 2 \times 2$ supercell with wurtzite structure (cf. Fig. 1). We then performed first-principles calculations to determine the relative energies of these five configurations with ionic optimization. To confirm the dynamical stability, phonon calculation was also performed to the optimized most stable structure to ensure the absence of negative frequencies in the crystal.[35–37]

Published under an exclusive license by AIP Publishing

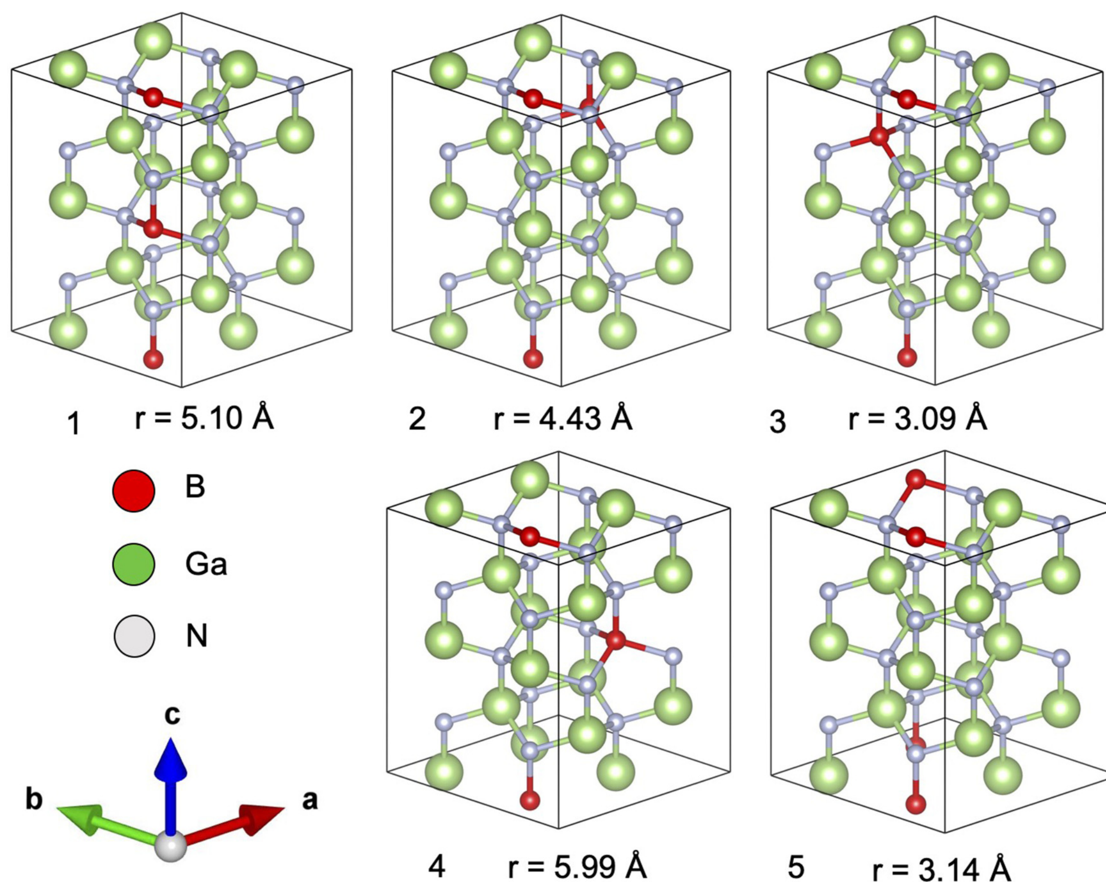

FIG. 1. Five geometric configurations of a $B_{0.125}Ga_{0.875}N$ system in a 2 × 2 × 2 supercell consisting of two B atoms (red spheres), 14 Ga atoms (green spheres), and 16 N atoms (gray spheres). The most stable configuration (panel 1) is obtained when two B atoms occupy Ga sites along the c-axis. $Al_{0.125}Ga_{0.875}N$ and $In_{0.125}Ga_{0.875}N$ also exhibit the same energetically favorable configuration. The interatomic distances between the two nearest-neighbor B atoms are also indicated with *r* in each configuration/panel.

III. RESULTS AND DISCUSSION

The most stable configurations of the $B_{0.125}Ga_{0.875}N$, $Al_{0.125}Ga_{0.875}N$, and $In_{0.125}Ga_{0.875}N$ system are obtained by comparing their total energies when two B, Al, or In atoms occupy different Ga sites in the wurtzite GaN crystal lattice. For $B_{0.125}Ga_{0.875}N$, the most stable configuration obtained is shown in Fig. 1, panel 1 where two B atoms occupy Ga sites located along the c-axis in the $2 \times 2 \times 2$ supercell. We have confirmed that this configuration still has the lowest energy when using a $4 \times 4 \times 4$ supercell (cf. Fig. S1 in the supplementary material) and when implementing a different exchange correlation functional (cf. Table S2 in the supplementary material). We compared the relative energy results using PBE and local-density approximation LDA exchange-correlation functionals and found the same energy trend. This energetically favorable configuration is also the same for $Al_{0.125}Ga_{0.875}N$ and $In_{0.125}Ga_{0.875}N$, where Al or In atoms occupy the Ga sites along the c-axis.

Although the other four geometric configurations shown in Fig. 1, panels 2–5 are realized rarely in the epitaxial growth of GaN-based ternary alloys, we assume that their probabilities can be estimated by the Boltzmann factor. Table I shows the in-plane and c-axis components of the interatomic distances between minority atoms before the structure optimization as well as the relative energies and the Boltzmann factors at defined growth temperatures for $B_{0.125}Ga_{0.875}N$, $Al_{0.125}Ga_{0.875}N$, and $In_{0.125}Ga_{0.875}N$ systems. The energy of the lowest energy configuration is set to zero and referred to as configuration 1. The other configurations 2–5 are sorted by their relative energies. $B_{0.125}Ga_{0.875}N$ and $Al_{0.125}Ga_{0.875}N$ show the largest and least value of energy deviations among the five configurations, respectively. The Boltzmann factor is subsequently determined using the relative energies and the metalorganic vapor phase epitaxy (MOVPE) growth temperatures of 1300 K for $B_{0.125}Ga_{0.875}N$ and $Al_{0.125}Ga_{0.875}N$ and 1050 K for $In_{0.125}Ga_{0.875}N$. The MOVPE growth temperature was chosen since MOVPE is the typical growth technique of III-V ternary alloys.

Published under an exclusive license by AIP Publishing

TABLE I. Interatomic distances (components), relative energies, and Boltzmann factors of different configurations of $B_{0.125}Ga_{0.875}N$, $Al_{0.125}Ga_{0.875}N$, and $In_{0.125}Ga_{0.875}N$ systems in a 2 × 2 × 2 supercell. The energy of the lowest energy configuration (configuration 1) is set to 0 while the other configurations are sorted by their relative energies. In-plane components and c-axis components of the interatomic distance between minority atoms at the initial coordinates are normalized by the lattice constants *a* and *c*, respectively.

			$B_{0.125}Ga_{0.875}N$		$Al_{0.125}Ga_{0.875}N$		$In_{0.125}Ga_{0.875}N$	
Configuration	In-plane component (lattice constant *a*)	c-axis component (lattice constant *c*)	Relative energy (eV)	Boltzmann factor ($T = 1300$ K)	Relative energy (eV)	Boltzmann factor ($T = 1300$ K)	Relative energy (eV)	Boltzmann factor ($T = 1050$ K)
1	0	1	0	1	0	1	0	1
2	1.15	0.5	0.123	0.335	0.001	0.988	0.032	0.699
3	0.58	0.5	0.459	0.017	0.008	0.934	0.111	0.295
4	1	1	0.484	0.013	0.010	0.918	0.131	0.236
5	1	0	0.709	0.002	0.018	0.852	0.189	0.124

It can be assumed that the probability of a high-energy configuration can be estimated by the Boltzmann factor. As shown in Table I, it is energetically preferable for B atoms to occupy Ga sites along the c-axis in a collinear configuration having the least in-plane component among other configurations. A similar trend is found for Al and In atoms, but the variation of probability, relative to configuration 1 along the c-axis direction, is smaller than that of B atoms. This result implies that B atoms have a stronger influence on the configuration of a GaN-based ternary alloy compared to Al and In atoms. Although this is the case, it is interesting to note that the most stable configurations are still the same for all alloys, where the B, Al, or In atoms prefer to occupy Ga sites along the c-axis which is also the typical epitaxial growth direction. In addition, the simulation results indicate that the compositional pulling effect for GaN-based ternary alloys can be explained by the Boltzmann factor obtained using the relative energies of their geometric configurations and the temperature during epitaxial growth.

As shown in Table I, the $B_{0.125}Ga_{0.875}N$, $Al_{0.125}Ga_{0.875}N$, and $In_{0.125}Ga_{0.875}N$ systems have different relative energies for configurations 2–5. Having identified the lowest geometric configuration (configuration 1) hints a more stable geometry for a higher degree of crystallinity within GaN-based ternary alloys at a 12.5% concentration of minority atoms. This result suggests that GaN-based alloys with better crystallinity can be obtained if the B, Al, or In atoms should be incorporated and occupy sites along the c-axis. Comparing the relative energies for the highest energy configuration (configuration 5), $B_{0.125}Ga_{0.875}N$ manifests a relatively high energy at 0.709 eV, while $Al_{0.125}Ga_{0.875}N$ has the lowest with 0.018 eV. Similarly, $B_{0.125}Ga_{0.875}N$ shows the largest relative energy for configurations 2–4. It is important to know the origin of these differences in GaN-based ternary alloys with different minority atoms. Figure 2 illustrates the relationship between the absolute value of the lattice mismatch between GaN and the relative energies of configurations 2–5 of the $B_{0.125}Ga_{0.875}N$, $Al_{0.125}Ga_{0.875}N$, $In_{0.125}Ga_{0.875}N$ systems. The lattice mismatch is obtained by the a-axis lattice constant of the binary nitride compounds,[6,12] where Vegard's law applies for $(B, Al, In)_xGa_{1-x}N$. It is found that the in-plane lattice mismatch and relative energies show a strong correlation. This correlation is very similar to the bandgap bowing parameter of BGaN, AlGaN, and InGaN alloys vs the lattice mismatch reported by Ougazzaden *et al.*[12] BGaN alloys show a large energy dependence on the geometric configuration as well as the large bandgap bowing parameter. It is, therefore, suggested that the lattice mismatch with GaN influences the electronic properties and stability of GaN-based ternary alloys.

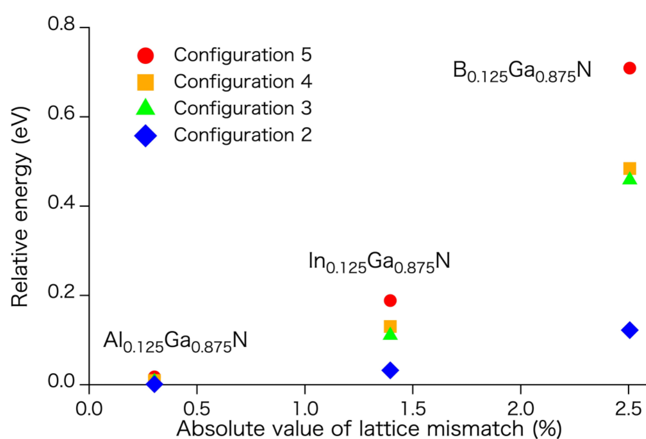

FIG. 2. Relative energies of configurations 2–5 of $B_{0.125}Ga_{0.875}N$, $Al_{0.125}Ga_{0.875}N$, and $In_{0.125}Ga_{0.875}N$ systems as a function of the absolute value of their lattice mismatch with GaN.

To further examine the $B_{0.125}Ga_{0.875}N$ system, Fig. 3 illustrates the nearest-neighbor bond length distributions between B and N atoms (positive value) and between Ga and N atoms (adjacent to the B atom, negative value) in a relaxed wurtzite $B_{0.125}Ga_{0.875}N$ structure with different geometric configurations. Figure 3 (lower left) indicates the histogram of bond lengths for configuration 1 (the most stable structure), while others indicate those for higher energy configurations. Pristine BN and GaN binary compounds have two kinds of nearest-neighbor bond lengths between B or Ga and N atoms. B and N atoms have bond lengths of 1.568–1.583 Å in BN (orange line), while Ga and N atoms have bond lengths of 1.966–1.974 Å in GaN (green line). These bond lengths along the c-axis direction are longer than the others. In the case of configuration 1 of $B_{0.125}Ga_{0.875}N$, the bond lengths between B and N atoms show an opposite trend and the bond length along the c-axis

Published under an exclusive license by AIP Publishing

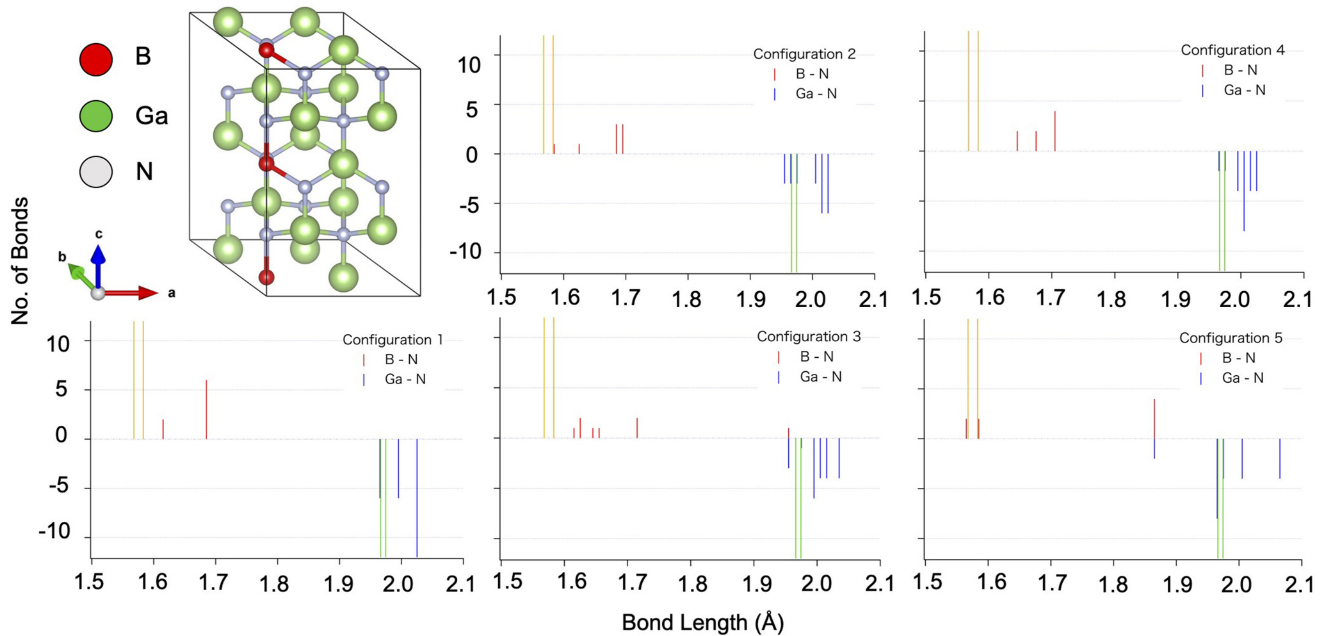

FIG. 3. Nearest-neighbor bond length distribution between B and N atoms (positive, red line) and between Ga and N atoms adjacent to B (negative, blue line) in a relaxed wurtzite $B_{0.125}Ga_{0.875}N$ structure with different geometric configurations (1–5). For comparison, the bond lengths of B and N atoms in BN and Ga and N atoms in GaN are also shown using orange and green lines, respectively. The average B–N and Ga–N bond lengths with the corresponding standard deviations are shown in Table S1 in the supplementary material.

direction is shorter than the others. From configuration 1 to configuration 5, the distribution of the nearest-neighbor bond lengths in $B_{0.125}Ga_{0.875}N$ becomes more dispersed or approaches values similar to those of binary BN and GaN compounds.

As mentioned earlier, the structural strain gives rise to the compositional pulling effect that affects the fabricated epitaxial layer. This strain in the grown epitaxial layer cannot be removed completely due to the limitation of compensation by interlayers. Different multinary alloys are fabricated as heterostructure devices, but the atomic radii of each constituent element of the heterostructures are intrinsically different. Inatomi *et al.* investigated the influence of the strain by thermodynamic analysis and showed that compressive and tensile strains cause an opposite trend of compositional pulling effect.[38] Meanwhile, Grandjean *et al.* performed Monte Carlo simulation considering the binding energies among constituent elements to investigate the surface segregation process.[39] Thus, the macroscopic approach and model calculation are effective for exploring the compositional pulling effect. However, investigations on the nanoscale origin of its atomistic mechanisms by first-principles calculations have not been performed yet. Therefore, our results reveal important insights into the spatial relationship between minority atoms and their effect on the wurtzite GaN-based alloy crystal structure. $B_{0.125}Ga_{0.875}N$, $Al_{0.125}Ga_{0.875}N$, and $In_{0.125}Ga_{0.875}N$ show the same trend on the preferential Ga-site substitution along the c-axis as well as the dependence of the geometric configuration on relative energies. The lattice mismatch and the order of relative energies between the minority atoms ($B > In > Al$) also show correspondence with the crystallinity of fabricated multinary alloys. As we have pointed out, AlGaN manifests a relatively low TDD compared to InGaN and AlBGaN layers. From these results, it is possible to conclude that the configuration of minority atoms in wurtzite GaN influences the compositional pulling effect in GaN-based ternary alloys. At this moment, the relationship between the geometric configuration of B atoms and the structural influence in BGaN alloys has yet to be clarified experimentally and requires further investigation.

IV. CONCLUSION

Using first-principles calculations, an atomistic origin of composition pulling effect was clarified from the geometric configurations of $B_{0.125}Ga_{0.875}N$, $Al_{0.125}Ga_{0.875}N$, and $In_{0.125}Ga_{0.875}N$ systems. In all GaN-based ternary alloys, the most stable configuration involves two B, In, or Al atoms occupying Ga sites in wurtzite GaN along the c-axis, which is the typical epitaxial growth direction. Among the five configurations considered, in-plane configurations have large relative energies, and the differences in these energies influence composition pulling effect because the in-plane direction is normal to the c-axis. $B_{0.125}Ga_{0.875}N$ has higher relative energies than $Al_{0.125}Ga_{0.875}N$ and $In_{0.125}Ga_{0.875}N$, which can be associated with the lattice mismatch with GaN. In addition, the compositional pulling effect for the GaN-based ternary alloys can

Published under an exclusive license by AIP Publishing

be well explained by obtaining the Boltzmann factor using the relative energy of the geometric configurations and the temperature during epitaxial growth. Moreover, for $B_{0.125}Ga_{0.875}N$, it is shown that the interatomic distances of B atoms affect defect formation wherein smaller distances result in greater bond length deviations, which imply greater structural deformation. In summary, our results reveal the energetically favorable configurations of $B_{0.125}Ga_{0.875}N$, $Al_{0.125}Ga_{0.875}N$, and $In_{0.125}Ga_{0.875}N$ and the bond deformations that manifest within these GaN-based ternary alloy crystal structures. As it is difficult for current experimental techniques to locate the atomic configuration of minority atoms, such a theoretical approach becomes indispensable. We have also shown the existence of non-degenerate configurations of III-nitride ternary alloys that causes compositional pulling effect. These results allow us to provide an insight into better conditions for crystal growth and eventually lead to more precise control for materials design.

SUPPLEMENTARY MATERIAL

See the supplementary material for details of the average B–N and Ga–N bond lengths and the simulation reliability.

ACKNOWLEDGMENTS

This work was supported by the Korea Institute of Science and Technology (Grant Nos. 2Z05840 and 2E31201), the Joint Usage/Research Center for Interdisciplinary Large-scale Information Infrastructures (JHPCN) (Project jh190019), the High-Performance Computing Infrastructure (HPCI) (Project Nos. hp190014, hp190111, and hp200040), the GIMRT Program of the Institute for Materials Research, Tohoku University (Proposal Nos. 20S0508 and 202012-SCKXX-0026), and the Japanese Ministry of Education, Culture, Sports, Science and Technology (MEXT) through the Program for Creation of Research Platforms and Sharing of Advanced Research Facilities (Photon Beam Platform).

DATA AVAILABILITY

The data that support the findings of this study are available within the article and its supplementary material.

REFERENCES

[1]M. R. Krames, O. B. Shchekin, R. Mueller-Mach, G. O. Mueller, L. Zhou, G. Harbers, and M. G. Craford, J. Disp. Technol. **3**, 160 (2007).
[2]H. Cotal, C. Fetzer, J. Boisvert, G. Kinsey, R. King, P. Hebert, H. Yoon, and N. Karam, Energy Environ. Sci. **2**, 174 (2009).
[3]S. Mokkapati and C. Jagadish, Mater. Today **12**, 22 (2009).
[4]R. Kudrawiec and D. Hommel, Appl. Phys. Rev. **7**, 041314 (2020).
[5]J. A. del Alamo, Nature **479**, 317 (2011).
[6]I. Vurgaftman and J. R. Meyer, J. Appl. Phys. **89**, 5815 (2001).
[7]H. Hirayama, J. Appl. Phys. **97**, 091101 (2005).
[8]M. Kneissl, T. Kolbe, C. Chua, V. Kueller, N. Lobo, J. Stellmach, A. Knauer, H. Rodriguez, S. Einfeldt, Z. Yang, N. M. Johnson, and M. Weyers, Semicond. Sci. Technol. **26**, 014036 (2010).
[9]J. J. Wierer Jr, A. David, and M. M. Megens, Nat. Photonics **3**, 163 (2009).
[10]M. T. Hardy, D. F. Feezell, S. P. DenBaars, and S. Nakamura, Mater. Today **14**, 408 (2011).
[11]E. Zdanowicz, D. Iida, L. Pawlaczyk, J. Serafinczuk, R. Szukiewicz, R. Kudrawiec, D. Hommel, and K. Ohkawa, J. Appl. Phys. **127**, 165703 (2020).
[12]A. Ougazzaden, S. Gautier, T. Moudakir, Z. Djebbour, Z. Lochner, S. Choi, H. J. Kim, J.-H. Ryou, R. D. Dupuis, and A. A. Sirenko, Appl. Phys. Lett. **93**, 083118 (2008).
[13]H. Amano, J. Phys.: Conf. Ser. **326**, 012002 (2011).
[14]T. Sugiyama, Y. Kuwahara, Y. Isobe, T. Fujii, K. Nonaka, M. Iwaya, T. Takeuchi, S. Kamiyama, I. Akasaki, and H. Amano, Appl. Phys. Express **4**, 015701 (2011).
[15]B. P. Gunning, M. W. Moseley, D. D. Koleske, A. A. Allerman, and S. R. Lee, J. Cryst. Growth **464**, 190 (2017).
[16]O. Rettig, J. P. Scholz, N. Steiger, S. Bauer, T. Hubáček, M. Zíková, Y. Li, H. Qi, J. Biskupek, U. Kaiser, K. Thonke, and F. Scholz, Phys. Status Solidi B **255**, 1700510 (2018).
[17]K. Hiramatsu, Y. Kawaguchi, M. Shimizu, N. Sawaki, T. Zheleva, R. F. Davis, H. Tsuda, W. Taki, N. Kuwano, and K. Oki, MRS Internet J. Nitride Semicond. Res. **2**, 6 (1997).
[18]T. Karasawa, K. Ohkawa, and T. Mitsuyu, J. Cryst. Growth **101**, 118 (1990).
[19]C. G. Van de Walle and J. Neugebauer, J. Appl. Phys. **95**, 3851 (2004).
[20]K. Liu, H. Sun, F. AlQatari, W. Guo, X. Liu, J. Li, C. G. Torres Castanedo, and X. Li, Appl. Phys. Lett. **111**, 222106 (2017).
[21]X. Hu, L. L. Kerr, X. Zhao, C. Ling, Z. Zhao, H. Jin, Y. Zhao, and J. Li, J. Alloys Compd. **798**, 112 (2019).
[22]R. Riane, Z. Boussahl, A. Zaoui, L. Hammerelaine, and S. F. Matar, Solid State Sci. **11**, 200 (2009).
[23]A. Kafi, F. D. Khodja, F. Saadaoui, S. Chibani, A. Bentayeb, and M. D. Khodja, Mater. Sci. Semicond. Proc. **113**, 105049 (2020).
[24]M. E. Turiansky, J.-X. Shen, D. Wickramaratne, and C. G. Van de Walle, J. Appl. Phys. **126**, 095706 (2019).
[25]A. Krytsos, M. Matsubara, and E. Belloti, Phys. Rev. B **99**, 035201 (2019).
[26]T. P. Mishra, G. J. Syaranamual, Z. Deng, J. Y. Chung, L. Zhang, S. A. Goodman, L. Jones, M. Bosman, S. Gradečak, S. J. Pennycok, and P. Canepa, Phys. Rev. Mater. **5**, 024605 (2021).
[27]W. Kohn and L. J. Sham, Phys. Rev. **140**, A1133 (1965).
[28]G. Kresse and J. Furthmüller, Phys. Rev. B **54**, 11169 (1996).
[29]G. Kresse and J. Furthmüller, Comput. Mater. Sci. **6**, 15 (1996).
[30]J. P. Perdew, K. Burke, and M. Ernzerhof, Phys. Rev. Lett. **77**, 3865 (1996).
[31]P. E. Blöchl, Phys. Rev. B **50**, 17953 (1994).
[32]G. Kresse and D. Joubert, Phys. Rev. B **59**, 1758 (1999).
[33]H. J. Monkhorst and J. D. Pack, Phys. Rev. B **13**, 5188 (1976).
[34]K. Momma and F. Izumi, J. Appl. Crystallogr. **44**, 1272 (2011).
[35]K. Parlinski, Z. Q. Li, and Y. Kawazoe, Phys. Rev. Lett. **78**, 4063 (1997).
[36]A. Togo and I. Tanaka, Scr. Mater. **108**, 1 (2015).
[37]K. Parlinski and Y. Kawazoe, Phys. Rev. B **60**, 15511 (1999)
[38]Y. Inatomi, Y. Kangawa, T. Ito, T. Suski, Y. Kumagai, K. Kakimoto, and A. Koukitu, Jpn. J. Appl. Phys. **56**, 078003 (2017).
[39]N. Grandjean, J. Massies, and M. Leroux, Phys. Rev. B **53**, 998 (1996).

Published under an exclusive license by AIP Publishing